LIMNOLOGY and OCEANOGRAPHY

ASLO

Limnol. Oceanogr. 9999, 2021, 1–13

doi: 10.1002/lno.11903

Elevated pCO_2 enhances under light but reduces in darkness the growth rate of a diatom, with implications for the fate of phytoplankton below the photic zone

Liming Qu,[1] John Beardall,[1,2] Xiaowen Jiang,[1] Kunshan Gao [1*]

[1]State Key Laboratory of Marine Environmental Science & College of Ocean and Earth Sciences, Xiamen University, Xiamen, China

[2]School of Biological Sciences, Monash University, Clayton, Australia

Abstract

Experimentally elevated pCO_2 and the associated pH drop are known to differentially affect many aspects of the physiology of diatoms under different environmental conditions or in different regions. However, contrasting responses to elevated pCO_2 in the dark and light periods of a diel cycle have not been documented. By growing the model diatom *Phaeodactylum tricornutum* under 3 light levels and 2 different CO_2 concentrations, we found that the elevated pCO_2/pH drop projected for future ocean acidification reduced the diatom's growth rate by 8–25% during the night period but increased it by up to 9–21% in the light period, resulting in insignificant changes in growth over the diel cycle under the three different light levels. The elevated pCO_2 increased the respiration rates irrespective of growth light levels and light or dark periods and enhanced its photosynthetic performance during daytime. With prolonged exposure to complete darkness, simulating the sinking process in the dark zones of the ocean, the growth rates decreased faster under elevated pCO_2, along with a faster decline in quantum yield and cell size. Our results suggest that elevated pCO_2 enhances the diatom's respiratory energy supplies to cope with acidic stress during the night period but enhances its death rate when the cells sink to dark regions of the oceans below the photic zone, with implications for a possible acidification-induced reduction in vertical transport of organic carbon.

Introduction

The oceans have absorbed approximately 30% (IPCC, 2014) of anthropogenically released CO_2, which remediates global warming but leads to ocean acidification (Sabine et al. 2004). Dissolution of CO_2 into seawater has already induced a global drop in pH of over 0.1 units (an increase of H^+ by more than 30%) since the end of the Industrial Revolution, and oceanic pH is predicted to decrease by 0.4 units (an increase of H^+ of more than 150%) by the end of the century when atmospheric CO_2 concentrations reach about 44.6 μM (1000 ppmv) (Caldeira and Wickett 2003; Gattuso et al. 2015). The biological effects of elevated CO_2 levels on phytoplankton have been the subject of intense investigation, using experimental manipulation of pCO_2 (and thus pH) in both natural mixed populations and in algal cultures, since it is of critical importance for our understanding of changes in the marine biological CO_2 pump. While a number of studies have shown that elevated pCO_2 projected for seeable future have positive effects on marine primary producers, especially in coastal waters, they can also be negatively impacted by the drop in pH (see the review by Gao et al. 2019 and literature therein), with differential responses to CO_2-induced ocean acidification even for the benthic algal calcifiers (Ries et al. 2009; Gao and Zheng 2010; Gattuso et al. 2015).

Diatoms populate a wide range of aquatic environments and have been shown to contribute about 40% of total marine primary production (Rousseaux and Gregg 2014). In marine environments, they dominate well-mixed coastal and upwelling regions (Malviya et al. 2016), being exposed to changing levels of light and CO_2/pH of different durations (Li et al. 2016*a*). The levels of light, temperature, and nutrients can bring about different effects of increased levels of pCO_2 on diatoms (Hama et al. 2016; Li et al. 2018; Gao et al. 2020). It is also well documented that diatoms (as well as other microalgae) show diel periodicity in cell division rates and other aspects of their physiology (Nelson and Brand 1979; Ashworth et al. 2013). Therefore, it is possible that elevated pCO_2 also exhibit differential effects on diatom cells in the light and dark periods of a diel cycle.

Whereas it is commonly recognized that elevated CO_2 levels, projected for the foreseeable future ocean, downregulate the

*Correspondence: ksgao@xmu.edu.cn

Additional Supporting Information may be found in the online version of this article.

CO_2 concentrating mechanisms of diatoms (Van de Waal et al. 2019). The acidic stress associated with increased pCO_2 imposes additional energy costs for maintenance of cellular homeostasis involving, for instance, changes in redox state, internal pH, and ion fluxes (Rokitta et al. 2012; Raven and Beardall 2020). Thus, the responses of diatoms to increased pCO_2 depend on the balance between positive effects of elevated CO_2 and negative effects of lowered pH (Gao and Campbell 2014; Hoppe et al. 2015; Seifert et al. 2020). While increased pCO_2 and consequent acidification is known to stimulate mitochondrial respiration by up to 30% to cope with the acidic stress in several diatoms (Wu et al. 2010; Yang and Gao 2012; Li et al. 2016*a*), it is expected that they might be affected more during dark periods under the influence of increased pCO_2, since respiratory CO_2 release during the night period can exacerbate the acidic stress within the diffusion boundary layer surrounding the cells (Flynn et al. 2012; Raven and Beardall 2020). Meanwhile, photosynthesis buffers the effects of increased pCO_2 via utilization of bicarbonate and subsequent neutralization of H^+ and provides energy for ATP-driven H^+ pumps (McNicholl et al. 2020). Thus, in the light period, the energy production from photosynthesis could outweigh the energy costs associated with the acidic stress due to elevated pCO_2 (Wu et al. 2010; Goldman et al. 2017). Therefore, here we hypothesize that diatom performance might be impaired at night and but be enhanced during daytime, leading to opposing effects on growth rate between day and night. On the other hand, in view of an average sinking speed of diatoms about 150 m d^{-1} (Iversen and Ploug 2013), diatoms may reach aphotic regions of the ocean within a couple of days, where they are exposed to a higher CO_2 and lower pH than in surface water (Cai et al. 2011; Laws and Maiti 2019). This raises a question on how changed seawater chemistry under elevated pCO_2 would affect diatoms when they have sunk to the aphotic zone, though some cells are still found alive down to 2000 m (Broman et al. 2017). Consequently, we further hypothesize that elevated pCO_2 may accelerate the rate of diatom death in dark regions of the oceans.

To test the above hypothesis, we grew the model diatom *Phaeodactylum tricornutum*, which has been shown to survive for up to 6 months in complete darkness (Antia and Cheng 1970), under experimentally increased pCO_2 conditions and different levels of light, and investigated its physiological performance and biochemical composition during light and dark periods of a diel cycle. We further examined growth and quantum yield in prolonged darkness and discuss the subsequent impacts of increased pCO_2 in the aphotic zone of the ocean.

Materials and Methods

Species and culture conditions

The diatom *Phaeodactylum tricornutum* Bohlin (strain CCMA 106), originally isolated from the South China Sea, was obtained from the Center for Collection of Marine Bacteria and Phytoplankton (CCMA) of Xiamen University. Cells were maintained at 20°C under a 12 h:12 h light and dark cycle in polycarbonate flasks and were grown in semicontinuous culture by regular dilution using 0.45 μm filtered natural seawater enriched with Aquil nutrients and vitamins (Morel et al. 1979). Cultures were exposed to ambient (410 ppmv, 18.3 μM) and elevated (1000 ppmv, 44.6 μM) CO_2 levels during growth. The CO_2 concentrations under ambient and elevated CO_2 conditions were achieved using ambient outdoor air or a mixture of pure CO_2 with ambient air in a CO_2 chamber (HP100G-D, Ruihua, China). The light was provided by white LEDs (with a wavelength range of 400–750 nm) in an incubator (Ruihua, China) and set up with three different levels: growth-saturating light (220 μmol photons m^{-2} s^{-1}), medium light (120 μmol photons m^{-2} s^{-1}), and growth-limiting light (50 μmol photons m^{-2} s^{-1}) (Zeng et al. 2020). All light intensities in this work were measured with a Solar Light sensor (PAM2100, USA). Sterile techniques were applied for all culturing and experimental manipulations. Cultures were maintained in exponential growth phase in sealed polycarbonate bottles by 24 h dilution. The initial cell concentration was 1×10^4 cells mL^{-1}, and the maximum cell concentration was controlled by the regular dilution to be below 2×10^5 cells mL^{-1} to minimize the impact of cell metabolism on seawater carbonate chemistry (Table 1). Triplicate independent cultures of acclimated cells were grown for at least 15 generations in each replicate for the different treatments before being used for determination of the physiological and biochemical parameters.

Experimental setup

We performed two sets of experiments: a light-dark cycle growth experiment (Exp. 1) and a prolonged darkness experiment (Exp. 2). In Exp. 1, cells which had been acclimated for more than 15 generations under the designated culture conditions were used for determinations of different parameters in the following generations (Fig. S1) after they had been kept in continuous darkness for 36 h to synchronize the cell division state (Li et al. 2016*b*). During the experiments, the cell concentration was maintained between 3×10^4 and 2×10^5 cells mL^{-1} by dilution every 24 h (Fig. S1). The cultures were sampled at 08:00 (immediately before light on) and 20:00 (immediately before light off) to obtain the parameters in the dark and light periods, respectively. Cell numbers and cell diameter were measured using a Z2 coulter counter (Beckman Coulter, USA). The specific growth rates (μ) were calculated using the following equation:

$$\mu\left(h^{-1}\right) = (\ln N_2 - \ln N_1)/(t_2 - t_1)$$

in which N_2 and N_1 represent cell concentrations at t_2 and t_1, which represent the time span of the light or dark period. The cell numbers were measured 30 min prior to the dark (19:30–20:00) or the light (07:30–08:00) periods.

In Exp. 2, following the cultures of Exp. 1, the cells were maintained in continuous complete darkness under the same culture conditions (except light), to simulate the "dark ocean" condition. For logistic reasons, we did not simulate the lowered temperature of the dark ocean. Physiological parameters were measured in the same way as in Exp. 1.

Seawater carbonate chemistry

To assure the stability of the carbonate systems in cultures, the pH_{NBS} values were measured prior to and after the daily dilution as well as in the middle of the light period using a pH meter, which was calibrated with NBS buffer. Total alkalinity (TA) was determined using the titration method (Lewis et al. 1998) and other parameters of the carbonate system were derived using the CO2SYS software based on pH and TA. Since the pH_{NBS} scale used with the standard buffers differs slightly from the pH_{Total} scale used by CO2SYS, a small correction was applied, using CO2SYS, to the measured pH_{NBS} values. The carbonate chemistry parameters are shown in Table 1.

Determination of photosynthetic rates

Net photosynthetic oxygen evolution and dark respiration rates were determined using a Clark-type oxygen electrode (Oxygraph, Hansatech, UK) at the experimental temperature. The respiration rates during the dark period (R_D) were measured before the lights were switched on (measurements began at 07:00 and finished before 08:00). Oxygen evolution rates were measured under the three different growth light levels, and respiratory rates in the light period (R_L) were measured in the middle of the photoperiod at the same time. Before measurements, samples were gently filtered (<0.02 MPa) onto cellulose acetate membranes, and then re-suspended into 20 mmol L^{-1} Tris-buffered media, which had been pre-adjusted to their responding culture media values. Buffer was used to avoid pH shifts during the oxygen exchange measurements with higher cell densities (3×10^5 to 5×10^5 cells mL^{-1}) than those used for growth. The pH levels were adjusted by adding hydrochloric acid or sodium hydroxide to the growth values (7.83 and 8.13) for the high- and low-CO_2 grown cells, respectively. The resuspended cells were injected into an oxygen electrode vessel with a magnetic stirrer held in a water-jacked chamber (for temperature control at 20°C). The dark respiration in the light phase and net O_2 evolution rates under the growth light levels were determined by covering the cuvette with a black box or by adjusting the distance from the light source (white LED), respectively.

Determination of pigment concentration

Sampling was carried out at 20:00. The cell suspensions (100 mL) were filtered onto GF/F filters under low vacuum pressure (<0.02 MPa) and soaked in methanol overnight at 4°C (Wellburn 1994). The extracts were centrifuged at $6000 \times g$ for 10 min to remove cell debris and glass fibers. The absorption spectra, from 400 to 800 nm, of the supernatant were measured with a spectrophotometer (DU 800, Beckman, USA). The chlorophyll *a* (Chl *a*) content of the supernatant was determined as follows:

$$\text{Chl}\,a\,(\text{mg mL}^{-1}) = 16.29 \times (A_{665} - A_{750}) - 8.54 \times (A_{652} - A_{750})$$

where A_{652}, A_{665}, and A_{750} represent absorbances of the methanol extracts at 665, 652, and 750 nm, respectively. Cellular Chl *a* was then determined from the volume of cell suspension filtered and its cell density.

Determination of chlorophyll *a* fluorescence

The photochemical parameters were determined using a Multi-Color PAM (Walz, Germany). Samples were harvested in the middle of the photoperiod. To assess the photochemical responses of cells grown in ambient and elevated CO_2

Table 1. Parameters of the seawater carbonate system under ambient (410 ppmv, 18.3 μM, AC) and elevated (1000 ppmv, 44.6 μM, HC) CO_2 concentrations during the semi-continuous cultures of the diatom *P. tricornutum* under three different light intensities (HL of 220, ML of 120 and LL of 50 μmol photons m^{-2} s^{-1}). Parameters were measured immediately before dilution of the cultures. Values are means ± SD of triplicate cultures. DIC = dissolved inorganic carbon, TA = total alkalinity. Different superscripted letters indicate significant ($p < 0.05$) differences among treatments. ACHL (ambient CO_2 and high light), HCHL (elevated CO_2 and high light), ACML (ambient CO_2 and medium light), HCML (elevated CO_2 and medium light), ACLL (ambient CO_2 and low light) and HCLL (elevated CO_2 and low light).

	pH_t	TA (μmol Kg^{-1})	DIC (μmol Kg^{-1})	HCO_3^- (μmol Kg^{-1})	CO_3^{2-} (μmol Kg^{-1})	CO_2 (μmol Kg^{-1})
ACHL	8.18 ± 0.03^a	2360.3 ± 11^a	2072.3 ± 15^a	1863.3 ± 7^a	195.9 ± 2^a	12.7 ± 1^a
HCHL	7.82 ± 0.02^b	2403.5 ± 15^a	2275.4 ± 13^b	2144.2 ± 12^b	97.1 ± 3^b	34.1 ± 1^b
ACML	8.14 ± 0.02^a	2413.9 ± 14^a	2098.1 ± 15^a	1887.6 ± 17^a	197.3 ± 6^a	13.2 ± 2^a
HCML	7.84 ± 0.03^b	2371.8 ± 11^a	2231.2 ± 5^b	2102.5 ± 11^b	95.1 ± 3^b	33.6 ± 2^b
ACLL	8.13 ± 0.04^a	2418.7 ± 19^a	2102.4 ± 9^a	1900.2 ± 22^a	189.4 ± 5^a	12.8 ± 1^a
HCLL	7.80 ± 0.04^b	2384.5 ± 13^a	2282.9 ± 23^b	2147.3 ± 13^b	100.2 ± 2^b	35.4 ± 1^b

Table 2. Summary of Two-way ANOVA analyses for interactive effects of pCO_2 and light intensity on growth rates of *P. tricornutum* during light (μ_L), dark (μ_D) periods and daily cycle (μ), net photosynthetic rate, mitochondrial respiration measured during light (R_L) and dark (R_D) periods, contents of chlorophyll *a* (Chl *a*), carotenoid (Car) and photochemical quantum yield. The symbol "*" indicates the interactions between factors, df = degrees of freedom, $F = F$ value, $P =$ values for significance level. The significant difference was set at $p < 0.05$.

Response variable	Factor variables	df	Mean Square	F	p
μ_D	pCO_2	1	0.005	0.097	0.757
μ_D	Light	2	0.526	11.058	<0.01
μ_D	pCO_2*Light	2	0.002	0.047	0.954
μ_L	pCO_2	1	0.005	0.097	0.757
μ_L	Light	2	0.526	11.059	<0.01
μ_L	pCO_2*Light	2	0.002	0.047	0.954
μ	pCO_2	1	0.005	0.097	0.757
μ	Light	2	0.526	11.059	<0.01
μ	pCO_2*Light	2	0.002	0.047	0.954
Net photosynthetic rate	pCO_2	1	390.437	1.592	0.221
Net photosynthetic rate	Light	2	3362.265	13.712	<0.01
Net photosynthetic rate	pCO_2*Light	2	2214.683	9.032	0.001
R_L	pCO_2	1	144.131	23.435	<0.01
R_L	Light	2	233.142	37.908	<0.01
R_L	pCO_2*Light	2	3.179	0.517	0.609
R_D	pCO_2	1	192.699	7.153	0.012
R_D	Light	2	323.669	12.015	<0.01
R_D	pCO_2*Light	2	2.775	0.103	0.902
F_v/F_m	pCO_2	1	1.027	0.609	0.451
F_v/F_m	Light	2	0.002	11.158	0.002
F_v/F_m	pCO_2*Light	2	<0.01	0.575	0.577
Yield	pCO_2	1	1.736	0.015	0.904
Yield	Light	2	0.017	14.149	4.699
Yield	pCO_2*Light	2	2.178	0.018	0.982
Chl *a*	pCO_2	1	0.124	18.223	<0.01
Chl *a*	Light	2	0.298	43.741	<0.01
Chl *a*	pCO_2*Light	2	0.028	4.171	0.025
Car	pCO_2	1	0.046	68.576	<0.01
Car	Light	2	0.093	137.951	<0.01
Car	pCO_2*Light	2	0.016	23.490	<0.01

concentrations and the changes of light, rapid light curves and maximum (F_v/F_m) and effective (F_v'/F_m') photochemical quantum yields were measured. Algae were dark adapted for 15 min before a light saturation pulse of >10,000 μmol photons m^{-2} s^{-1} was applied for 0.8 s to obtain F_m, before estimating rapid light curves. The maximum quantum yield of photosystem II (PSII) is given as $F_v/F_m = (F_m - F_o)/F_m$, where F_v is the difference between the maximum fluorescence (F_m) measured after the saturating light pulse and the minimum fluorescence (F_o) emitted as a result of the measuring light only. The effective photochemical quantum yields of PSII (hereafter referred to as yield) were determined according to yield $= (F_m' - F_t)/F_m'$ for light-adapted samples, where F_m' indicates maximum chlorophyll fluorescence of light-adapted samples and F_t indicates steady chlorophyll fluorescence of light-adapted samples. The yield was measured under actinic light intensity similar to the culture light levels. Rapid light curves were fitted to the following model: rETR (relative electron transfer rate) = PAR/ ($a \times PAR^2 + b \times PAR + c$), where PAR is the photon flux density of actinic light (μmol photons m^{-2} s^{-1}) and *a*, *b*, and *c* are model parameters. The assay light intensities were chosen and increased from 0 to 1723 μmol photons m^{-2} s^{-1} with 12 steps (0, 63, 121, 178, 264, 377, 516, 731, 964, 1214, 1327, 1723 μmol photons m^{-2} s^{-1}) and a duration of 15 s at each intensity. The light-harvesting efficiency (*a*), light saturation point (I_K), and maximum relative electron transport rate ($rETR_{max}$) were calculated from *a*, *b*, and *c* according to the equations in Eilers and Petters (1988).

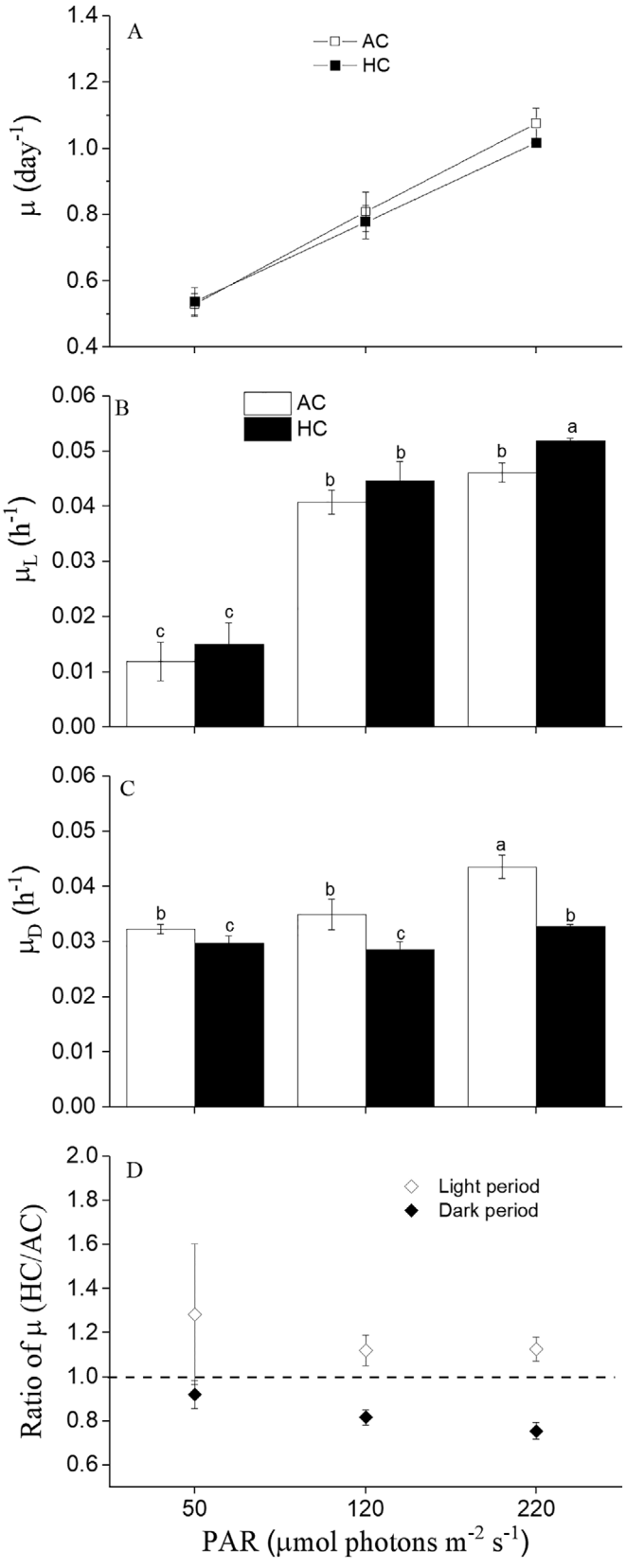

Prolonged darkness experiment

After placing the cultures in continuous darkness, we measured the specific growth rate of *P. tricornutum* per day (i.e. over a 24 h period) according to the equation given above (Section 2.2) and at the same time recorded the mean cell diameter of *P. tricornutum* using a Z2 counter.

The effective photochemical quantum yield (yield) of PSII was also determined according to the equation of Genty et al. (1989), using a Multi-Color PAM (Walz, Germany). Under dark growth conditions, 10 mL culture medium was taken and placed in the measuring cuvette, and a saturation pulse was given to the alga to measure the yield. The parameter was measured when the cultures were first transferred from the 12 L:12 D to the 24 D condition and the values recorded subsequently at 24 and 48 h.

Statistics

All data are shown as the means ± SD of three independent cultures. To test for significant differences between treatments, one-way analyses of variance (ANOVA), with post hoc tests were performed ($p = 0.05$). Two-way ANOVA was applied when examining the interactions between CO_2 and light. To test direct effects between two particular treatments standard t-tests (level of significance $p < 0.05$) were used. All statistical analyses were carried out with Origin 9.0 and presented in Table 2. Different letters in figures and tables indicate statistically different values between treatments based on post-hoc tests.

Results

Carbonate system

The carbonate chemistry parameters were stable, and the pH variation was less than 0.05 units within either the ambient and elevated CO_2 treatments (Table 1). Elevated pCO_2 did not alter TA, but increased the concentrations of DIC, pCO_2 and HCO_3^- by 6.1%, 62.7%, and 13.1%, respectively, and decreased CO_3^{2-} by 50.4% when compared to the ambient CO_2 concentration treatment under the high light condition. Light intensity for growth did not alter the carbonate system.

Fig. 1. The effect of light intensity and CO_2 concentration on specific growth rate of *P. tricornutum*. (**A**) Specific growth rates expressed as per day in a 24 h period (over the diel cycle), (**B**) specific growth rates per hour in the light period (from 08:00 to 20:00), (**C**) specific growth rates per h in the dark period (from 20:00 to 08:00 the next day), (**D**) the ratio of specific growth rates in elevated (HC) to ambient (AC) CO_2-grown cells. Different superscripted letters indicate significant ($p < 0.05$) differences among the treatments. The lines in (**A**) are the linear fitted daily growth rates vs growth light intensities, the fitting formulae are $y = 0.273 + 0.256x$ ($R^2 = 0.9998$, $p = 0.006$) for the AC condition, $y = 0.239 + 0.298x$ ($R^2 = 1$, $p < 0.001$) for the HC condition. Data are the means ± SD of triplicate cultures.

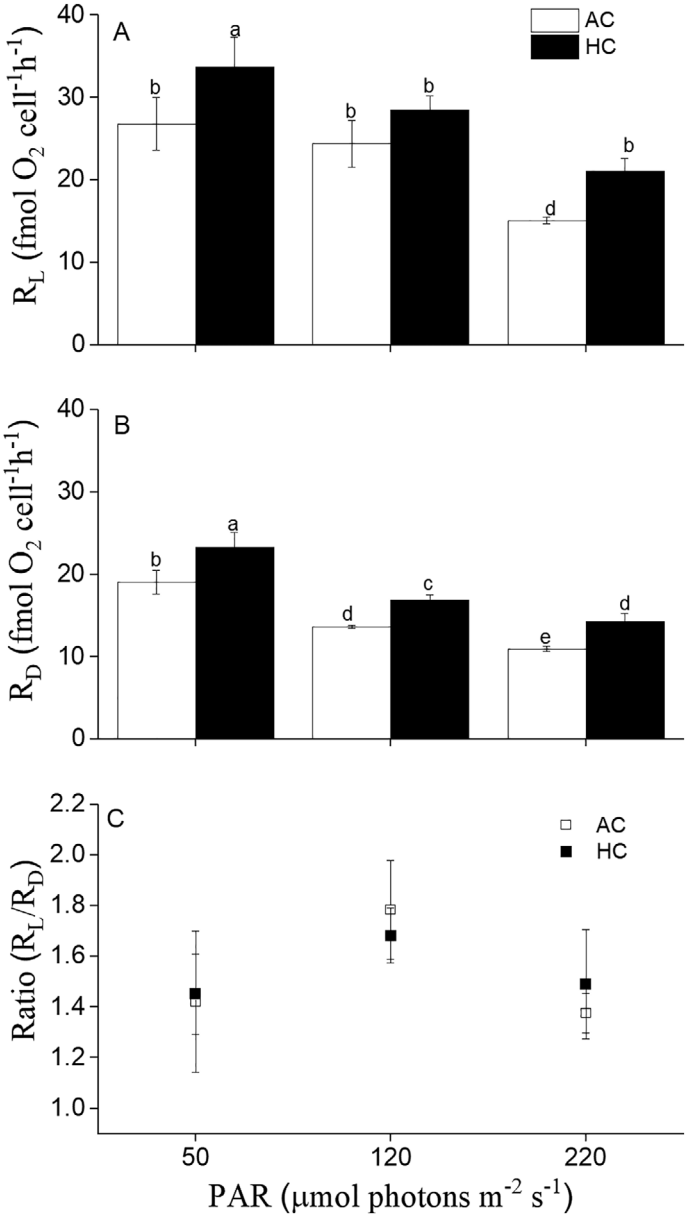

Fig. 2. The effect of light intensity and CO_2 concentration on respiration rates of *P. tricornutum*. (**A**) The respiration rate in the middle of the light period, (**B**) the respiration rate in the dark period (measured 1 h before the light period began), (**C**) the ratio of the respiration rate in the light period to that in the dark period. Different superscripted letters indicate significant ($p < 0.05$) differences among the treatments. AC indicates ambient CO_2 and HC the elevated CO_2 treatments. Data are the means ± SD of triplicate cultures.

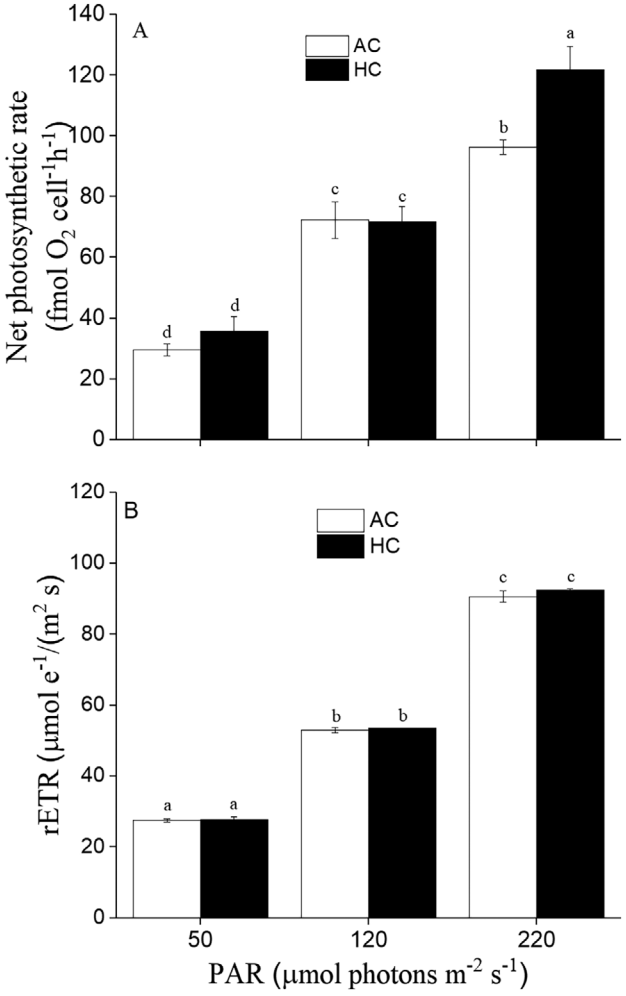

Fig. 3. The effect of light intensity and CO_2 concentration on oxygen evolution rates (**A**) and relative electron transport (**B**) of *P. tricornutum*. Different superscripted letters indicate significant ($p < 0.05$) differences among the treatments. AC indicates ambient CO_2 and HC the elevated CO_2 treatments. Data are the means ± SD of triplicate cultures.

Specific growth rate

Over a 24 h period (light vs dark), the growth rate of *P. tricornutum* was strongly dependent on light intensity, but there was no significant difference ($p = 0.76$) in growth rate between the ambient and elevated pCO_2 treatments (Fig. 1A). In the light period, increased pCO_2 enhanced the growth rate by about 11.1% ($p = 0.31$), 8.7% ($p = 0.17$), and 21.3% ($p = 0.005$) for cells grown under low, medium, and high light conditions, respectively (Fig 1B). However, the growth rates in the dark period were less dependent on growth light levels (Fig. 1C), significantly decreased the growth rate in the dark period by about 7.9% ($p = 0.047$), 18.5% ($p = 0.02$), and 25.2% ($p = 0.001$) for cells grown under low, medium and high light conditions, respectively (Table 2). The ratios of growth rate under elevated to ambient CO_2 concentrations in were higher than 1 in the light period but lower than 1 during night, reflecting that increased pCO_2 promoted in the light period but inhibited the growth of *P. tricornutum* (Fig. 1D). The mean cell diameter increased with increased growth light intensities in the light period, and increased pCO_2 resulted in a decrease at any tested light intensity (Fig. S3A). The cell

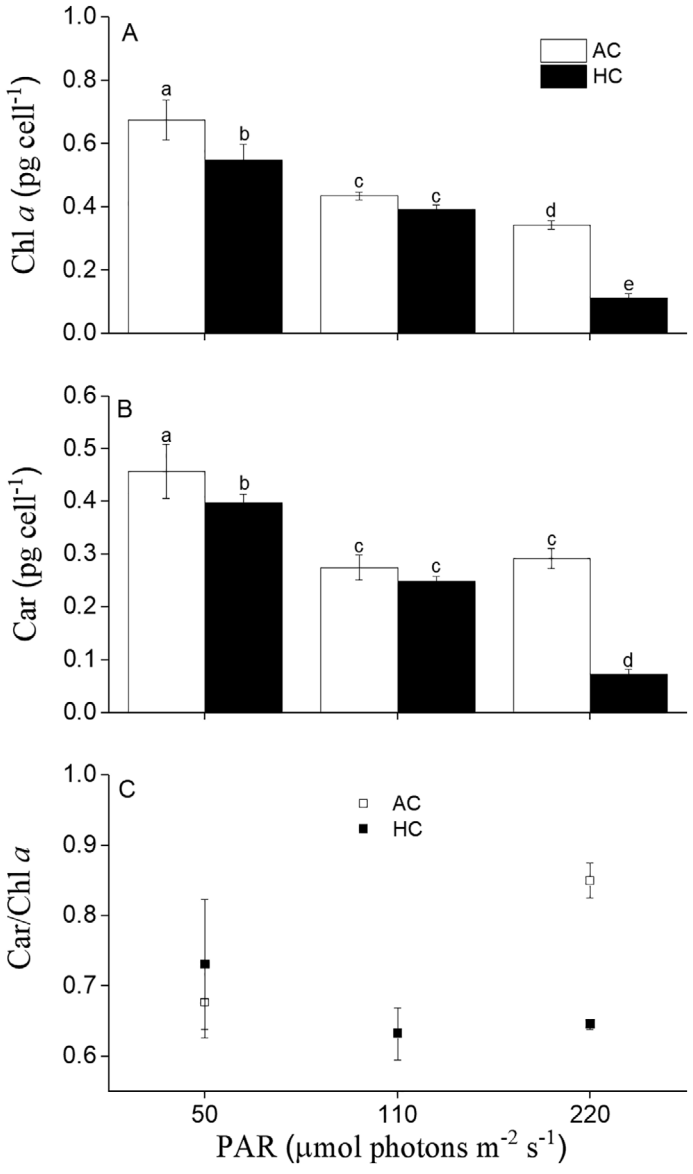

Fig. 4. The effect of light intensity and CO_2 concentration on cellular contents of pigments of *P. tricornutum*. (**A**) Chlorophyll *a* (Chl *a*), (**B**) carotenoids (Car), and (**C**) the ratio of Car to Chl *a*. Different superscripted letters indicate significant ($p < 0.05$) differences among the treatments. AC indicates ambient CO_2 and HC the elevated CO_2 treatments. Data are the means ± SD of triplicate cultures.

diameter in the elevated CO_2-grown cells was smaller in the light period regardless of the growth light levels, as reflected by the diameter ratios of ambient to elevated CO_2-grown cells, and the cells grown under low light and high CO_2 showed the smallest diameter during light period (Fig. S3B).

Photosynthetic and respiratory activities

The mitochondrial respiration rates of *P. tricornutum* determined during light period (R_L) increased under the increased pCO_2 at any growth light intensity. Light intensity and CO_2 concentration had no interactive effect on respiration rate in the light period (Fig. 2A, Table 2). The respiration during night (R_D) showed a similar trend to R_L, being significantly increased with increased pCO_2, by about 18.2% ($p = 0.006$), 19.2% ($p = 0.0006$), and 22.9% ($p = 0.03$) under low, medium, and high light conditions, respectively (Fig. 2B). The ratios of R_L/R_D were greater than 1 under the three different culture light intensities as R_L values were always higher than R_D, though increased pCO_2 had statistically insignificant effect on the ratio regardless of the light intensity (Fig. 2C). The net photosynthetic rate was the highest under the high light condition, and it increased by about 24.9% ($p = 0.03$) and by 69.3% ($p = 0.0002$) relative to medium and low light levels, respectively. Increased pCO_2 significantly enhanced the net photosynthetic rate by about 20.9% ($p = 0.005$) under the high light condition (Fig. 3A).

Pigment contents

The contents of Chl *a* varied under the different light intensities and increased with the decreased light intensities under both CO_2 concentrations. Increased pCO_2 resulted in decreased Chl *a* under all light conditions, in particular, it decreased the content of Chl *a* by about 66.9% ($p = 0.0002$) under the high light condition (Fig. 4A). The carotenoid contents (Car) showed a similar trend to Chl *a* (Fig. 4B). Increased pCO_2 significantly decreased the ratio of carotenoid to Chl *a* under the high light condition ($p = 0.004$), but had no significant differences on cells under the medium and low light conditions ($p = 0.64$, Fig. 4C).

Photochemical parameters

The relative electron transport rates (rETR) increased with growth light intensity, but increased pCO_2 had no statistically significant effect under any of the growth light level (Fig. 3B). The maximal rETR values of *P. tricornutum* under high light level were about 36.2% and 72% higher than in medium and low light condition, respectively, with yield being decreased with increasing growth light intensities (Table S1). The dark-adapted maximum PSII quantum yield (F_v/F_m) values were not affected either by the culture light and increased pCO_2 ($p = 0.45$) (Table S1). Increased pCO_2 did not give rise to significant effects on $rETR_{max}$ under high light but enhanced it under low light condition (Fig. S2, Table S1). The light-harvesting efficiency (*a*) was enhanced with decreasing growth light intensities, though increased pCO_2 had no significant effect on this parameter across all three light intensities (Table S1).

Parameters in the prolonged darkness

The specific growth rates of *P. tricornutum* decreased rapidly with prolonged darkness (Fig. 5), reached zero in about 48 h (Fig. 5A). Increased pCO_2 decreased the growth rate as reflected by the ratios of elevated to ambient CO_2

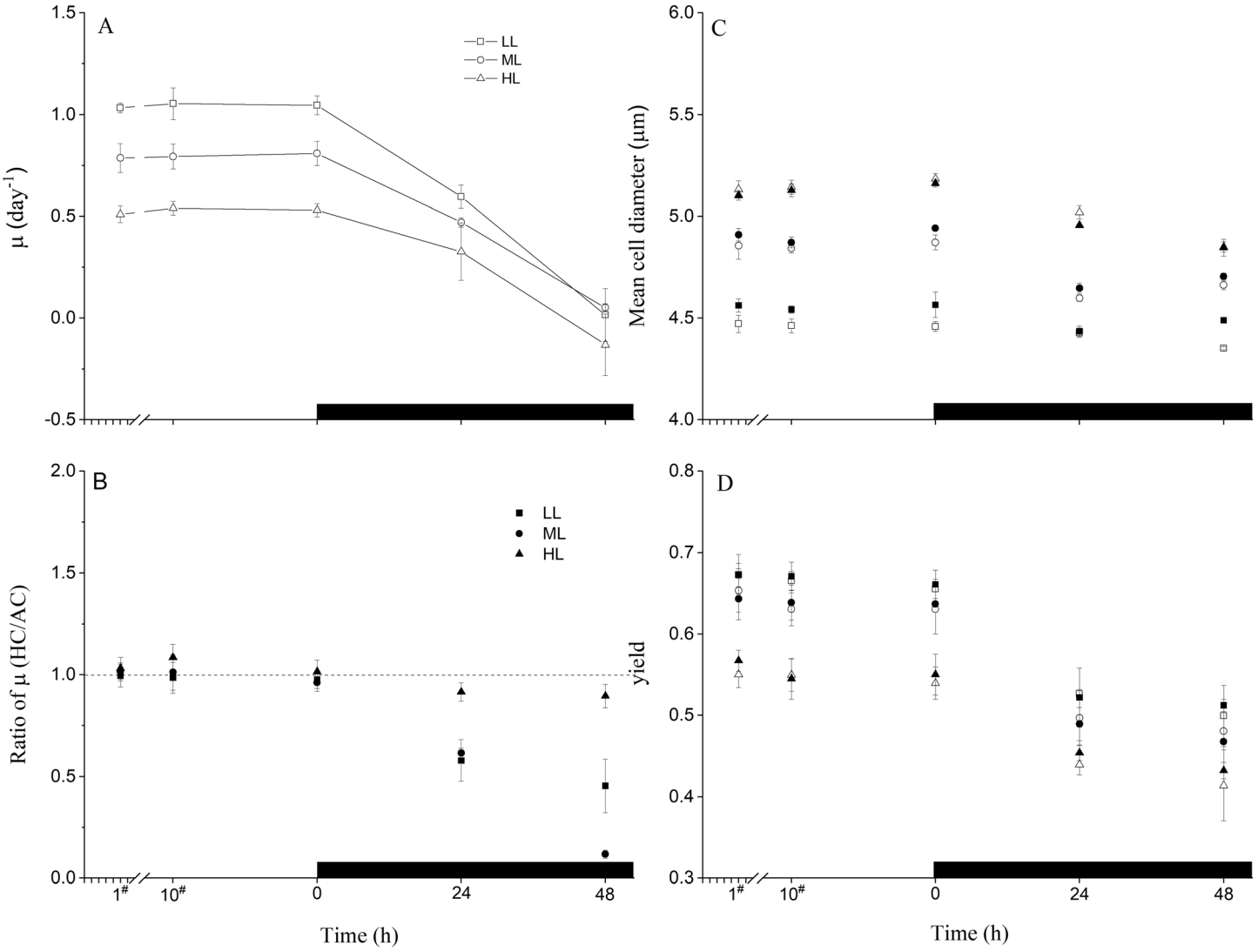

Fig. 5. Changes in growth rate, cell size and photochemical quantum yield of *P. tricornutum* grown under a normal light and dark cycle (12 L:12 D) at 3 light intensities and then transferred to prolonged darkness conditions (shown as the dark bars). (**A**) Specific growth rate under ambient CO_2 condition; (**B**) the ratio of specific growth rate under elevated (HC) to that under ambient (AC) CO_2; (**C**) the mean cell diameter and (**D**) the photochemical quantum yield under AC and HC. The "0" indicates the start of the prolonged darkness treatment. The gap between $1^{\#}$ and $10^{\#}$ in the x-coordinate indicates that cells had been grown for over10 generations under each of the treatments before the darkness treatments. The open and solid squares represent ACLL (ambient CO_2 and low light) and HCLL (elevated CO_2 and low light), respectively; the open and solid cycles represent ACML (ambient CO_2 and medium light) and HCML (elevated CO_2 and medium light), respectively; the open and solid triangles represent ACHL (ambient CO_2 and high light) and HCHL (elevated CO_2 and high light), respectively.

treatments, which were less than 1 (Fig. 5B). The mean cell diameter decreased with prolonged darkness under the ambient CO_2 condition, and with larger diameters of the cells grown at the higher light intensity (Fig. 5C). Increased pCO_2 barely altered the cell diameter under medium and low light conditions.

There was no significant change in the yield value over time during the prolonged darkness treatment between the ambient and elevated CO_2 conditions, and yield was maintained at high values in the dark period for cells previously grown under all three different light intensities. However, the values of yield in cells previously grown under low and medium light were higher than that in high light during the prolonged dark period (Fig. 5D).

Discussion

It is well known that the cell division rates of microalgae vary across a diel cycle, with peaks occurring for some species in the dark period but in others during daytime, though there are a few species that show no discernable pattern in growth rate (Eppley et al. 1971; Nelson and Brand 1979; Ashworth

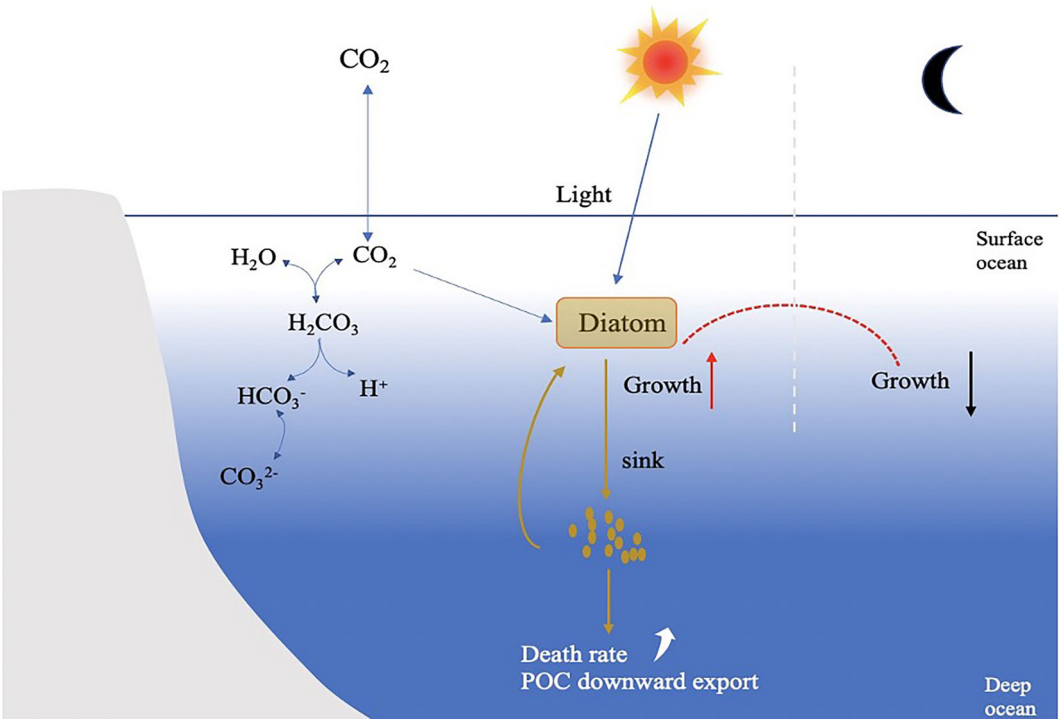

Fig. 6. Illustration of the potential effects of elevated pCO_2 on diatoms under light and dark periodicity, based on our data for *P. tricornutum*. Under influence of elevated pCO_2, the growth rate decreases in the dark period, but increases under light. In addition, elevated pCO_2 leads to a faster decline in relative growth rates of cells under prolonged darkness due to enhanced respiration caused by the acidic-stress, implying that diatom cells sinking to the depths below the photic zone die faster with increased pCO_2.

Table 3. Documented specific growth rates (μ) of *P. tricornutum* grown under different light, temperature and CO_2 conditions. T indicates temperature, "N" no significant effect of elevated pCO_2, "U" unknown result, "+" elevated pCO_2 increased the growth rate, "−" elevated pCO_2 decreased the growth rate.

Light level (μmol photons m^{-2} s^{-1})	Photoperiod	*T* (°C)	Medium	Effect on μ	Strain	Reference
120	14L:10D	20	Aquil	+	CCMA106	Wu et al. 2010
70	12L:12D	20	Aquil	+	CCMA106	Li et al. 2012*b*
sunlight	N	20	Aquil	N	CCMA106	Li et al. 2015
70	12L:12D	20	Aquil	N	CCMA106	Li et al. 2012*a*
60,200	12L:12D	20	Aqui	+, N	CCMA106	Li et al. 2014
150	12L:12D	20	Aquil	−, N	CCMA106	Li et al. 2017
216	12L:12D	22	f/2	−	Unknown	Bautista-Chamizo et al. 2018
150	12L:12D	20	Aquil	N	CCMP632	Huang et al. 2019*a*
100	12L:12D	20	f/2	+	IOCAS-001	Huang et al. 2019*b*
100	12L:12D	20	Aquil*	+	CCMP630	Shi et al. 2019
100	12L:12D	24	f/2	N	AF18	Quelhas et al. 2019
50,120	12L:12D	20,2520	f/2	N	Bohlin ac-2	Zeng et al. 2020
50,120,220	12L:12D	20	Aquil	N	CCMA106	Present work
50,120,220	Light period	20	Aquil	+, N	CCMA106	Present work
50,120,220	Dark period	20	Aquil	−	CCMA106	Present work

et al. 2013). In *P. tricornutum*, cells divide almost twice every 24 h under optimal light and temperature conditions (Fig. 1 in this work). This rapid growth enabled us to test our hypothesis that increased pCO_2 might have different impacts on cell division rates between daytime and night.

Our data showed that changed seawater chemistry under elevated pCO_2 projected for the end of this century inhibited growth rates of *P. tricornutum* during the night period but stimulated it during the light period. Increased pCO_2 sped up the decline in cell growth in prolonged darkness, accompanied by a faster decline in cell diameter and quantum yield (Figs. 5 and 6). However, the specific growth rates over a 24 h period (i.e., across a diel cycle) in *P. tricornutum* were linearly related to the growth light intensities, with insignificant difference in the growth rate per day at any given light intensity tested due to enhanced photosynthetic performances by the increased pCO_2 during light period. Obviously, the high CO_2-induced night-inhibition and daytime-enhancement of cell division are balanced to result in neutral effects over a diel cycle (Fig. 1). When the diatom *T. weissflogii* was grown under continuous light over periods up to 6 h, no significant changes in photosynthesis and growth rates were observed, though its respiration increased (Goldman et al. 2017). *P. tricornutum* (the same strain as used in this work) grown under light/dark cycle of 14:10 significantly increased its daily specific growth rate by 5.4% under elevated pCO_2 at the same level of this work (Wu et al. 2010). In the present work, *P. tricornutum* had been grown with 12 h:12 h light and dark cycle, which exhibited reduced growth rate in dark period. The difference in growth response to the increased pCO_2 between the present and Wu et al. (2010), after being acclimated to more than 15 generations, could be attributed to different time spans of light period (14 vs 12 h). It is reasonable to attribute the discrepancy to the acclimation spans and absence and/or shortened dark periods, which has been suggested to lessen the acidic stress to the cells, which is exacerbated during night periods (Flynn et al. 2012, Figs 1, 2). There have been 12 published papers on the growth response of *P. tricornutum* to increased pCO_2 (Table 3), with stimulative, neutral and negative effects all being documented, which may be due to the contrastingly opposing effects of increased pCO_2 during light and dark periods under different levels of nutrient and light treatments employed as well as the use of different strains.

The specific growth rates of *P. tricornutum* showed different results in the light and dark periods under different light conditions (Fig. 1). It has been suggested that timing of cell division in diatoms across light-dark cycles may be related to other environmental factors (Ashworth et al. 2013) and here we have shown that availability of CO_2 and pH changes can be a driver influencing the cell division rate and timing, as reflected in the opposing impacts of increased pCO_2 on its growth rate (Fig. 1). The observation that increased pCO_2 had contrasting effects on the growth of the diatom in the light and dark periods, being stimulatory during daytime and inhibitory during night (Figs 1,6), could be attributed to the microenvironmental changes near the cell surface (Flynn et al. 2012). Considering the chemical environment within the diffusion boundary layers surrounding the cells, CO_2 uptake and bicarbonate utilization via CO_2 concentrating mechanisms (CCMs) during photosynthesis can buffer the acidic stress resulting from elevated pCO_2. However, in darkness, respiratory CO_2 release can exacerbate the acidic stress to further drop the pH within the diffusion boundary layers, thereby leading to extra energy costs at the sacrifice of growth rate. With buffering effects within the diffusion boundary layers from photosynthetic CO_2 removal, elevated CO_2 availability can down regulate CO_2 concentrating mechanisms and save the operational energy cost, consequently enhancing growth and carbon fixation in the light period (Hopkinson et al. 2011; Reinfelder 2011; Hurd 2015). In the dark period or dark regions of the oceans, the release of CO_2 due to the increased pCO_2 enhanced respiration would further reduce pH within the diffusion boundary layers (Hurd et al. 2009). In the diatom *Thalassiosira pseudonana*, elevated pCO_2 was demonstrated to increase dark respiration as well (Laws et al. 2020). Therefore, increased pCO_2 could aggravate acidification stress in the dark period and regions below photic zones, leading to enhanced loss of particulate carbon. All in all, the opposing effects of increased pCO_2 between daytime and night can result in different directions of acidification impacts, depending on the levels of other interacting factors, such as daylength, nutrient availability and temperature (Gao et al. 2019).

In general, phytoplankton in different ecological niches are likely to have different responses to the environmental changes (Laws 1991; Xiao et al. 2019). In the present work, the physiological characteristics of the diatom showed contrasting differences among the treatments of growth light, CO_2 and prolonged darkness. Due to mixing by water motion and seasonal variations in natural environments, diatom cells are exposed to other ecological niches, especially the shift to prolonged or complete dark environments (Long et al. 2011). Here our data suggest that diatom cells decrease growth, yield and cell size, and die faster under the influence of increased pCO_2 in prolonged darkness (Fig. 6), which was shown to significantly decrease nuclear transcriptional activity in diatoms (Nymark et al. 2013), though they can rapidly respond when exposed to light (Broman et al. 2017). In the vertical ocean environments, CO_2 concentration increases with depth (Laws and Maiti 2019) along with lower water temperature in the aphotic zone. Temperature may alter the extent of the effects observed in the diatom cells under the prolonged darkness, mimicking the sinking process in the dark ocean. Since lower temperature would lead to lower respiration rate, the increased pCO_2 induced impact during darkness observed here could be less under lowered temperatures.

In conclusion, our results clearly support the hypothesis that elevated pCO_2 can have opposing effects on the growth

rates of diatoms between night and daytime periods and also accelerates the death of diatoms in the dark oceans (Fig. 6). Nevertheless, marine diatoms are widespread across the different latitudes and governed by a multitude of environmental cycles which include not only the daily day-night cycle, but also cycles with shorter or longer periods such as tides, lunar/semi-lunar cycles or seasons. Prolonged night period during winter has been showed to give rise to growth inhibition under influenced of increased pCO_2 in the diatom of *Skeletonema costatum* (Li et al. 2021), which could be due to negative effects of elevated pCO_2/pH drop during night (as shown in the present work). It is also worth noting that any opposing effects of increased pCO_2 on diatoms and other microalgae across a day/night cycle might also be influenced by nutrient availability, limitation of which has been shown to enhance respiration under elevated pCO_2 (Li et al. 2018). Consequently, it is expected that increased pCO_2 induced growth inhibition in diatoms during the night period can be magnified when warming and nutrient limitation are coexisting drivers.

References

Antia, N. J., and J. Y. Cheng. 1970. The survival of axenic cultures of marine planktonic algae from prolonged exposure to darkness at 20°C. Phycologia **9**: 179–183. doi:10.2216/i0031-8884-9-2-179.1

Ashworth, J., S. Coesel, A. Lee, E. V. Armbrust, M. V. Orellana, and N. S. Baliga. 2013. Genome-wide diel growth state transitions in the diatom *Thalassiosira pseudonana*. Proc. Natl. Acad. Sci. U. S. A. **110**: 7518–7523. doi:10.1073/pnas.1300962110

Bautista-Chamizo, E., A. R. Borrero-Santiago, M. R. De Orte, Á. Delvalls, and I. Riba. 2018. Effects of CO_2 enrichment on two microalgae species: A toxicity approach using consecutive generations. Chemosphere **213**: 84–91. doi:10.1016/j.chemosphere.2018.09.001

Broman, E., V. Sachpazidou, M. Dopson, and S. Hylander. 2017. Diatoms dominate the eukaryotic metatranscriptome during spring in coastal "dead zone" sediments. Proc. R. Soc. B **284**: 20171617. doi:10.1098/rspb.2017.1617

Cai, W. J., and others. 2011. Acidification of subsurface coastal waters enhanced by eutrophication. Nat. Geosci. **4**: 766–770. doi:10.1038/ngeo1297

Caldeira, K., and M. E. Wickett. 2003. Oceanography: Anthropogenic carbon and ocean pH. Nature **425**: 365–365. doi:10.1038/425365a

Eilers, P. H. C., and J. C. H. Petters. 1988. A model for the relationship between light intensity and the rate of photosynthesis in phytoplankton. Ecol. Model. **42**: 199–215. doi:10.1016/0304-3800(88)90057-9

Eppley, R. W., J. B. Rogers, J. McCarthy, and A. Sournia. 1971. Light/dark periodicity in nitrogen assimilation of the marine phytoplankters *Skeletonema costatum* and *Coccolithus huxleyi* in N-limited chemostat culture. J. Phycol. **7**: 150–154. doi:10.1111/j.1529-8817.1971.tb01494.x

Flynn, K. J., and others. 2012. Changes in pH at the exterior surface of plankton with ocean acidification. Nat. Clim. Change **2**: 510–513. doi:10.1038/nclimate1696

Gao, K. S., J. Beardall, D.-P. Häder, P. Hall-Spencer, J. M. Gao, and D. A. Hutchins. 2019. Effects of ocean acidification on marine photosynthetic organisms under the concurrent influences of warming, UV radiation and deoxygenation. Front. Mar. Sci. **6**: 322. doi:10.3389/fmars.2019.00322

Gao, K. S., and D. A. Campbell. 2014. Photophysiological responses of marine diatoms to elevated CO_2 and decreased pH: a review. Funct. Plant Biol. **41**: 449–459. doi:10.1071/FP13247

Gao, K. S., G. Gao, Y. Wang, and S. Dupont. 2020. Impacts of ocean acidification under multiple stressors on typical organisms and ecological processes. Mar. Life Sci. Technol. **2**: 279–291. doi:10.1007/s42995-020-00048

Gao, K. S., and Y. Zheng. 2010. Combined effects of ocean acidification and solar UV radiation on photosynthesis, growth, pigmentation and calcification of the coralline alga *Corallina sessilis* (Rhodophyta). Global Change Biol. **16**: 2388–2398. doi:10.1111/j.1365-2486.2009.02113.x

Gattuso, J. P., and others. 2015. Contrasting futures for ocean and society from different anthropogenic CO_2 emissions scenarios. Science **349**: aac4722. doi:10.1126/science.aac4722

Genty, B., J.-M. Briantais, and N. R. Baker. 1989. The relationship between the quantum yield of photosynthetic electron transport and quenching of chlorophyll fluorescence. BBA-GEN. Subjects. **990**: 87–92. doi:10.1016/S0304-4165(89)80016-9

Goldman, J., M. L. Bender, and F. M. M. Morel. 2017. The effects of pH and pCO_2 on photosynthesis and respiration in the diatom *Thalassiosira weissflogii*. Photosynth. Res. **132**: 83–93. doi:10.1007/s11120-106-0330-2

Hama, T., T. Inoue, R. Suzuki, H. Kashiwazaki, S. Wada, D. Sasano, N. Kosugi, and M. Ishii. 2016. Response of a phytoplankton community to nutrient addition under different CO_2 and pH conditions. J. Oceanogr. **72**: 207–223. doi:10.1007/s10872-015-0322-4

Hopkinson, B. M., C. L. Dupont, A. E. Allen, and F. M. M. Morel. 2011. Efficiency of the CO_2-concentrating mechanism of diatoms. Proc. Natl. Acad. Sci. U. S. A. **108**: 3830–3837. doi:10.2307/41061021

Hoppe, C. J. M., L. M. Holtz, S. Trimborn, and B. Rost. 2015. Ocean acidification decreases the light-use efficiency in an Antarctic diatom under dynamic but not constant light. New Phytol. **207**: 159–171. doi:10.1111/nph.13334

Huang, A., S. Wu, W. Gu, Y. Li, X. Xie, and G. Wang. 2019*b*. Provision of carbon skeleton for lipid synthesis from the breakdown of intracellular protein and soluble sugar in *Phaeodactylum tricornutum* under high CO_2. BMC Biotechnol. **19**: 1–18. doi:10.1186/s12896-019-0544-4

Huang, R., J. Ding, K. S. Gao, M. H. Cruz de Carvalho, L. Tirichine, C. Bowler, and X. Lin. 2019*a*. A potential role for epigenetic processes in the acclimation response to elevated pCO_2 in the model diatom *Phaeodactylum tricornutum*. Front. Microbiol. **9**: 3342. doi:10.3389/fmicb.2018.03342

Hurd, C. L. 2015. Slow-flow habitats as refugia for coastal calcifiers from ocean acidification. J. Phycol. **51**(4): 599–605. doi:10.1111/jpy.12307

Hurd, C. L., C. D. Hepburn, K. I. Currie, J. Raven, and K. A. Hunter. 2009. Testing the effects of ocean acidification on algal metabolism: considerations for experimental designs. J. Phycol. **45**: 1236–1251. doi:10.1111/j.1529-8817.2009.00768.x

IPCC. 2014. Climate change 2014: Synthesis report. Geneva: IPCC, p. 1–151.

Iversen, M. H., and H. Ploug. 2013. Temperature effects on carbon-specific respiration rate and sinking velocity of diatom aggregates—potential implications for deep ocean export processes. Biogeosciences **10**: 4073–4085. doi:10.5194/bg-10-4073-2013

Laws, E. A. 1991. Photosynthetic quotients, new production and net community production in the open ocean. Deep-Sea Res. A **38**: 143–167. doi:10.1016/0198-0149(91)90059-O

Laws, E. A., and K. Maiti. 2019. The relationship between primary production and export production in the ocean: Effects of time lags and temporal variability. Deep-Sea Res. I **148**: 100–107. doi:10.1016/j.dsr.2019.05.006

Laws, E. A., S. A. Mcclellan, and U. Passow. 2020. Interactive effects of CO_2, temperature, irradiance, and nutrient limitation on the growth and physiology of the marine diatom *Thalassiosira pseudonana* (Coscinodiscophyceae). J. Phycol. **56**: 1614–1624. doi:10.1111/jpy.13048

Lewis, E., D. Wallace, and L. J. Allison. 1998. Program developed for CO_2 system calculations, ORNL/CDIAC-105. Oak Ridge, TN: US Department of Energy, Carbon Dioxide Information Analysis Center, Oak Ridge National Laboratory.

Li, F., J. Beardall, S. Collins, and K. S. Gao. 2017. Decreased photosynthesis and growth with reduced respiration in the model diatom *Phaeodactylum tricornutum* grown under elevated CO_2 over 1800 generations. Global Change Biol. **23**: 127–137. doi:10.1111/gcb.13501

Li, F., J. Beardall, and K. S. Gao. 2018. Diatom performance in a future ocean: Interactions between nitrogen limitation, temperature, and CO_2-induced seawater acidification. ICES J. Mar. Sci. **61**: 1535–1563. doi:10.1093/icesjms/fsx239

Li, F., Y. Wu, D. A. Hutchins, F. Fu, and K. S. Gao. 2016*a*. Physiological responses of coastal and oceanic diatoms to diurnal fluctuations in seawater carbonate chemistry under two CO_2 concentrations. Biogeosciences **13**: 6247–6259. doi:10.5194/bg-13-6247-2016

Li, H., T. Xu, J. Ma, F. Li, and J. Xu. 2021. Physiological responses of Skeletonema costatum to the interactions of seawater acidification and combination of photoperiod and temperature. Biogeosciences. **18**: 1439–1449. doi:10.5194/bg-18-1439-2021

Li, M., X. Shi, C. Guo, and S. Lin. 2016*b*. Phosphorus deficiency inhibits cells division but not growth in the dinoflagellate *Amphidinium carterae*. Front. Microbiol. **7**: 8261–10. doi:10.3389/fmicb.2016.00826

Li, W., K. S. Gao, and J. Beardall. 2012*a*. Interactive effects of ocean acidification and nitrogen-limitation on the diatom *Phaeodactylum tricornutum*. Plos One. **7**: e51590. doi:10.1371/journal.pone.0051590

Li, W., K. S. Gao, and J. Beardall. 2015. Nitrate limitation and ocean acidification interact with UV-B to reduce photosynthetic performance in the diatom *Phaeodactylum tricornutum*. Biogeosciences **12**: 2383–2393. doi:10.5194/bg-12-2383-2015

Li, Y., K. S. Gao, E. V. Villafañe, and E. W. Helbling. 2012*b*. Ocean acidification mediates photosynthetic response to UV radiation and temperature increase in the diatom *Phaeodactylum tricornutum*. Biogeosciences **9**: 7197–7226. doi:10.5194/bg-9-3931-2012

Li, Y., J. Xu, and K. S. Gao. 2014. Light-modulated responses of growth and photosynthetic performance to ocean acidification in the model diatom *Phaeodactylum tricornutum*. PLoS One. **9**: e96173. doi:10.1371/journal.pone.0096173

Long, M. H., D. Koopmans, P. Berg, S. Rysgagrd, R. N. Glud, and D. H. Søgaard. 2011. Oxygen exchange and ice melt measured at the ice-water interface by eddy correlation. Biogeosciences **9**: 1957–1967. doi:10.5194/bg-9-1957-2012

Malviya, S., and others. 2016. Insights into global diatom distribution and diversity in the world's ocean. Proc. Natl. Acad. Sci. U. S. A. **113**: 201509523. doi:10.1073/pnas.1509523113

McNicholl, C., M. S. Koch, P. W. Swarzenski, F. R. Oberhaensli, A. Taylor, M. G. Batista, and M. Metian. 2020. Ocean acidification effects on calcification and dissolution in tropical reef macroalgae. Coral Reefs. **39**: 1635–1647. doi:10.1007/s00338-020-01991-x

Morel, F. M. M., J. G. Rueter, D. M. Anderson, and R. R. L. Guillard. 1979. Aquil: A chemically defined phytoplankton culture medium for trace metal studies. J. Phycol. **15**: 135–141. doi:10.1111/j.1529-8817.1979.tb02976.x

Nelson, D. M., and L. E. Brand. 1979. Cell division periodicity in 13 species of marine phytoplankton on a light: dark cycle1. J. Phycol. **15**: 67–75. doi:10.1111/j.1529-8817.1979.tb02964.x

Nymark, M., K. Valle, C. Hancke, K. Winge, P. Andresen, K. Johnsen, G. Bones, and T. Brembu. 2013. Molecular and photosynthetic responses to prolonged darkness and subsequent acclimation to re-illumination in the diatom Phaeodactylum tricornutum. Plos One. **8**: e58722. doi:10.1371/journal.pone.0058722

Quelhas, P. M., and others. 2019. Industrial production of *Phaeodactylum tricornutum* for CO_2 mitigation: Biomass productivity and photosynthetic efficiency using photobioreactors of different volumes. J. Appl. Phycol. **31**: 2187–2196. doi:10.1007/s10811-019-1750-0

Raven, J., and J. Beardall. 2020. Energizing the plasmalemma of marine photosynthetic organisms: the role of primary active transport. J. Mar. Bio. Assoc. UK. **100**: 1–14. doi:10.1017/s00253154200000211

Reinfelder, J. R. 2011. Carbon concentrating mechanisms in eukaryotic marine phytoplankton. Annu. Rev. Mar. Sci. **3**: 291–315. doi:10.1146/annurev-marine-120709-142720

Ries, J. B., A. L. Cohen, and D. C. McCorkle. 2009. Marine calcifiers exhibits mixed responses to CO_2-induced ocean acidification. Geology **37**: 1131–1134. doi:10.1130/G30210A.1

Rokitta, S. D., U. John, and B. Rost. 2012. Ocean acidification affects redox-balance and ion-homeostasis in the life-cycle stages of *Emiliania huxleyi*. PLoS One. **7**: e52212. doi:10.1371/journal.pone.0052212

Rousseaux, C. S., and W. W. Gregg. 2014. Interannual variation in phytoplankton primary production at a global scale. Remote Sens. **6**: 1–19. doi:10.3390/rs6010001

Sabine, C. L., and others. 2004. The oceanic sink for anthropogenic CO_2. Science **305**: 367–371. doi:10.1126/science.1097403

Seifert, M., B. Rost, S. Trimborn, and J. Hauck. 2020. Meta-analysis of multiple driver effects on marine phytoplankton highlights modulating role of pCO_2. Global Change Biol. **26**: 1–18. doi:10.1111/gcb.15341

Shi, D., H. Hong, X. Su, L. Liao, S. Chang, and W. Lin. 2019. The physiological response of marine diatoms to ocean acidification: Differential roles of seawater pCO_2 and pH. J. Phycol. **55**: 521–533. doi:10.1111/jpy.12855

Van de Waal, D. B., Brandenburg, K. M. Keuskamp, J. Trimborn, S. Rokitta, S. Kranz, S. A. and Rost, B. 2019. Highest plasticity of carbon-concentrating mechanisms in earliest evolved phytoplankton. Limno. Oceanogr. Lett. **4**: 37-43. doi:10.1002/lol2.10102

Wellburn, A. R. 1994. The spectral determination of chlorophylls a and b, as well as total carotenoids, using various solvents with spectrophotometers of different resolution. J. Plant Physiol. **144**: 307–313. doi:10.1016/S0176-1617(11)81192-2

Wu, Y., K. S. Gao, and U. Riebesell. 2010. CO_2-induced seawater acidification affects physiological performance of the marine diatom *Phaeodactylum tricornutum*. Biogeosciences **7**: 2915–2923. doi:10.5194/bg-7-2915-2010

Xiao, W., E. A. Laws, Y. Xie, L. Wang, X. Liu, J. Chen, B. Chen, and B. Huang. 2019. Responses of marine phytoplankton communities to environmental changes: new insights from a niche classification scheme. Water Res. **166**: e115070. doi:10.1016/j.watres.2019.115070

Yang, G. Y., and K. S. Gao. 2012. Physiological responses of the marine diatom *Thalassiosira pseudonana* to increased pCO_2 and seawater acidity. Mar. Environ. Res. **79**: 142–151. doi:10.1016/j.marenvres.2012.06.002

Zeng, X., and others. 2020. Light alters the responses of two marine diatoms to increased warming. Mar. Environ. Res. **154**: 104871. doi:10.1016/j.marenvres.2019.104871

Acknowledgments

The study was supported by National Natural Science Foundation of China (41720104005, 41890803, 41721005). The authors are grateful to the laboratory engineers Xianglan Zeng, Wenyan Zhao and to the PhD students, He Li, and Qianqian Fu for their logistic and technical supports.

Conflict of interest

The authors declare that they have no conflict of interest.

Submitted 08 March 2021
Revised 26 April 2021
Accepted 26 June 2021

Associate editor: Ilana Berman-Frank